

Shi, Y., Thrippleton, M. J., Blair, G. W., Dickie, D. A. , Marshall, I., Hamilton, I., Doubal, F. N., Chappell, F. and Wardlaw, J. M. (2018) Small vessel disease is associated with altered cerebrovascular pulsatility but not resting cerebral blood flow. *Journal of Cerebral Blood Flow and Metabolism*, (doi:[10.1177/0271678X18803956](https://doi.org/10.1177/0271678X18803956)).

This is the author's final accepted version.

There may be differences between this version and the published version. You are advised to consult the publisher's version if you wish to cite from it.

<http://eprints.gla.ac.uk/171834/>

Deposited on: 22 May 2019

Title: Small vessel disease is associated with altered cerebrovascular pulsatility but not resting cerebral blood flow

Running title: Intracranial pulsatility and CBF in SVD

Yulu Shi, MBChB, PhD <sup>1,2,3</sup>; Michael J. Thrippleton, PhD <sup>3,4</sup>; Gordon W. Blair, BSc (Hons), MBChB, MRCP <sup>3,4</sup>; David Alexander Dickie, PhD <sup>3,5</sup>; Ian Marshall, PhD <sup>3,4</sup>; Iona Hamilton <sup>3</sup>; Fergus N. Doubal, MBChB, FRCP, PhD <sup>3</sup>; Francesca Chappell, PhD <sup>3</sup>; Joanna M. Wardlaw, MBChB, MD, FRCR <sup>3,4,6\*</sup>

<sup>1</sup> Department of Neurology, Zhongnan Hospital, Wuhan University, Wuhan, China; <sup>2</sup> Department of Neurology, Tiantan Hospital, Beijing, China; <sup>3</sup> Brain Research Imaging Centre, Centre for Clinical Brain Sciences, University of Edinburgh, Edinburgh, UK; <sup>4</sup> UK Dementia Research Institute at The University of Edinburgh, Edinburgh Medical School, Edinburgh, UK; <sup>5</sup> Institute of Cardiovascular and Medical Sciences, University of Glasgow, Glasgow, UK; <sup>6</sup> Centre for Cognitive Ageing and Cognitive Epidemiology, University of Edinburgh, Edinburgh, UK.

\*Corresponding author: Professor Joanna M. Wardlaw, Centre for Clinical Brain Science, University of Edinburgh, 49 Little France Crescent, Edinburgh EH16 4SB, UK; telephone: +44 (0)131 537 2943; fax: +44 (0)131 537 2661; e-mail: joanna.wardlaw@ed.ac.uk.

**Word count:** Abstract (200/200), Manuscript (5273/6000)

**Tables:** 4

**Figures:** 3 (2 color figures)

## **Abstract** (200/200)

Cerebral small vessel disease (SVD) contributes to 25% of ischemic strokes and 45% of dementias. We aimed to investigate the role of cerebral blood flow (CBF) and intracranial pulsatility in SVD. We scanned 60 patients with minor ischemic stroke, representing a range of white matter hyperintensities (WMH). We rated WMH and perivascular spaces (PVS) using semi-quantitative scales and measured WMH volume. We measured flow and pulsatility in the main cerebral vessels and cerebrospinal fluid (CSF) using phase-contrast MRI. We investigated the association between flow, pulsatility and SVD features. In 56/60 patients (40 male,  $67.8 \pm 8.3$  years) with complete data, median WMH volume was 10.7mL (range 1.4-75.0mL), representing median 0.77% (0.11-5.17%) of intracranial volume. Greater pulsatility index (PI) in venous sinuses was associated with larger WMH volume (e.g. superior sagittal sinus,  $\beta=1.29$ ,  $P<0.01$ ) and more basal ganglia PVS (e.g. odds ratio=1.38, 95% confidence interval 1.06, 1.79, per 0.1 increase in superior sagittal sinus PI) independently of age, sex and blood pressure. CSF pulsatility and CBF were not associated with SVD features. Our results support a close association of SVD features with increased intracranial pulsatility rather than with low global CBF, and provide potential targets for mechanistic research, treatment and prevention of SVD.

**Keywords:** cerebral blood flow, cerebrovascular pulsatility, MRI, white matter hyperintensities, perivascular spaces, cerebral small vessel disease, stroke

## 1 Introduction

2 Cerebral small vessel disease (SVD) is closely related to stroke and dementia.<sup>1</sup> 25% of ischemic strokes are  
3 lacunar (or small vessel) in type.<sup>2</sup> Indeed, patients with a history of stroke, regardless of the aetiology, had  
4 significantly higher burden of white matter hyperintensities (WMH) than those without.<sup>3</sup> Presence of SVD also  
5 increases the risk of future stroke. SVD also accounts for 45% of dementias<sup>4</sup> and WMH are associated with  
6 cognitive decline.<sup>1</sup> Thus, understanding the mechanism of SVD is essential for preventing stroke and dementia.  
7 Reduced cerebral blood flow (CBF) has been widely proposed as the cause of SVD. However, the cross-  
8 sectional association between reduced CBF and WMH in small studies was weaker in larger studies,<sup>5</sup> especially  
9 when accounting for age or dementia diagnosis; in large longitudinal studies, high WMH predicted subsequent  
10 lower CBF, not the reverse.<sup>6</sup>

11 Vascular stiffening may be an alternative contributor to SVD.<sup>7</sup> Aging and vascular risk factors are associated  
12 with loss of arterial elasticity.<sup>8,9</sup> It has been hypothesised that the stiffened vessels would be less able to dampen  
13 pressure and pulsatility, leading to more pulsatile energy dissipating in the brain leading to tissue damage.<sup>10,11</sup>  
14 Cerebral veins and CSF are also thought to be important compartments for compensating arterial pulse  
15 pressure.<sup>11</sup> An excessive, poorly dampened pulse transmitted into the arterioles, capillaries, CSF or veins, could  
16 damage the brain.<sup>11</sup>

17 Some clinical studies have shown that high pulsatility in the internal carotid or middle cerebral arteries (ICA,  
18 MCA) is associated with WMH.<sup>12-14</sup> However, in these studies, pulsatility was assessed in one (or at most two)  
19 main cerebral arteries by ultrasound.<sup>15</sup> Very few studies assessed pulsatility in the arteries, veins and CSF  
20 contemporaneously in the same subjects,<sup>16</sup> limiting the clinical evidence.

21 Furthermore, perivascular spaces (PVS) around the arterioles and venules are increasingly realised to play a  
22 fundamental role in SVD. PVS become enlarged and visible on MRI in patients with hypertension, and are  
23 associated with WMH and lacunar stroke,<sup>17,18</sup> with inflammation<sup>19</sup> and dementia.<sup>20</sup> Normal cerebrovascular  
24 pulsatility has been identified as a key factor in facilitating fluid drainage from the interstitium to the PVS and  
25 thence to the extracerebral CSF and venous system.<sup>21</sup> However, so far, no clinical studies have measured cranial  
26 vascular pulsatility and PVS visibility.<sup>15</sup>

27 Pulse-gated phase-contrast MRI is able to detect flow and pulsatility in major cerebral vessels and CSF spaces.  
28 It showed higher venous pulsatility in patients with vascular dementia,<sup>16</sup> and altered CSF pulsatility in the

aqueduct in patients with age-related depression,<sup>22</sup> compared to healthy volunteers. However, these studies were small, any association between pulsatility and SVD may simply reflect co-association with age or risk factors. In this study, we measured pulsatility and CBF in the major cerebral arteries, veins and CSF spaces using phase-contrast MRI in patients with SVD features who presented with minor ischemic stroke. We assessed the relationship between the haemodynamic indices and WMH and PVS, and hypothesised that increased intracranial pulsatility, rather than low CBF, would be associated with SVD independently of age and blood pressure.

## **Method**

### **Patient recruitment**

We recruited patients prospectively with symptomatic minor (i.e. non-disabling) ischemic stroke presenting to the NHS Lothian Stroke Service (median onset-to-study-visit time 92 days, range 32-1768 days) who were not cognitively impaired. NHS Lothian covers three major hospitals and is managed by one centralised team of stroke physicians. Diagnosis and classification of stroke were based on the combination of clinical presentation and appearance on MR brain imaging with diffusion-weighted (DWI) and other relevant diagnostic sequences, and was carefully cross-checked by a panel of experts in stroke (FD and JMW). ‘Non-disabling’ was defined as not requiring assistance in activities of daily living. We excluded patients with disabling stroke, poorly-controlled diabetes mellitus (type II diabetes requiring insulin), poorly-controlled hypertension (systolic blood pressure >220 or diastolic > 110 mmHg), chronic kidney disease (eGFR <30 mL/min/1.73m<sup>2</sup>), chronic respiratory disease, angina or heart failure, a known family history of intracranial aneurysm, subarachnoid haemorrhage, arteriovenous malformation, any psychiatric illness that would limit compliance with study procedures (including mild cognitive impairment and dementia), and those with contraindications to MRI.

Written informed consent was obtained from all participants. The study was conducted following the UK Health Research Authority Research Ethics Committee approvals (ref. 14/EM/1126) and according to the principles expressed in the Declaration of Helsinki.

### **Imaging protocols**

All participants were imaged on the same 1.5 Tesla MRI scanner (Signa HDxt, General Electric, Milwaukee, WI) using an 8-channel phased-array head coil). We acquired velocity images using a 2-D cine phase-contrast pulse sequence with retrospective peripheral pulse gating using sequences that are similar to those in previous studies.<sup>23, 24</sup> Vascular flow (TR/TE=9/5 ms, 25° flip angle, 256 x 128 matrix, 2 signal averages) was determined in the distal cervical ICA, vertebral arteries, and internal jugular veins axially, superior to the carotid bifurcation where the ICA walls are parallel (**Figure 1**). We measured venous sinus flow (TR/TE=9/5 ms (approx.), 25° flip angle, 256 x 128 matrix, 2 signal averages) in the superior sagittal sinus, straight sinus, and transverse sinuses. A coronal-oblique slice that intersected the superior sagittal sinus at 2cm above the torcular and through the midpoint of straight sinus was selected. We also measured CSF flow through slices perpendicular to the cerebral aqueduct (TR/TE=11/6.5 ms (approx.), 20° flip angle, 256 x 256 matrix, 2 signal averages) and axially at C2-C3 level (TR/TE=11/7 ms (approx.), 20° flip angle, 256 x 128 matrix, 3 signal averages). All velocities were measured at 32 time points during the cardiac cycle, with velocity coding value set to 70 cm/s for neck arteries, 50 cm/s for brain sinuses, 10 cm/s for aqueduct CSF, and 6 cm/s for cervical CSF. Views per segment were set to 2 in all phase-contrast MRI scans. We acquired structural images including T1-weighted, T2-weighted, fluid attenuation inversion recovery (FLAIR) and gradient-echo (GRE) images using the acquisitions that we have reported previously.<sup>25</sup>

## **Peripheral hemodynamic measurements**

In order to assess the vessel stiffness in peripheral circulation, we also measured carotid-radial pulse wave velocity (PWV) and aortic augmentation index using a tonometry device (SphygmoCor, Sydney, Australia) in a supine position. We obtained sequential recordings of radial and carotid artery pressure waveforms via a transducer with a small sensor. We measured the distances from the suprasternal notch to the carotid and radial artery sampling sites and calculated the difference between the two distances. We then calculated PWV as the ratio of the distance in meters to the transit time in seconds. We also obtained the aortic pressure waveform and aortic augmentation index (AIx) automatically from the device using a generalized transfer function to correct for upper limb pressure amplification. AIx was calculated as the aortic augmentation pressure divided by aortic pulse pressure which was then normalised to a heart rate of 75 bpm.

## **Image processing**

### *Structural imaging analysis*

All imaging analysts (DAD, MJT, YS, JMW) were blinded to patients' clinical data and haemodynamic measures generated from phase-contrast MRI. Structural image acquisitions were co-registered within each subject.<sup>26</sup> WMH were automatically calculated by validated software which first registered diffeomorphically a cohort-specific white matter probability map to each subject using T1W image data.<sup>27</sup> This provided a "clean" estimate of the white matter for each subject, e.g., a white matter surface without gaps/holes created by WMH. Hyperintense outliers were identified on FLAIR by transforming each voxel to a standard (z) score.<sup>28</sup> Voxels with  $z \geq 1.5$  and within the estimated white matter surface were initially defined as WMH. Final WMH estimates were defined by 3D smoothing to reduce noise and account for partial volumes around WMH edges. WMH masks were then manually corrected for each participant and stroke lesions were excluded manually according to STRIVE guidelines<sup>17</sup> and supervision from an experienced neuroradiologist (JMW). A stroke lesion on FLAIR was defined as a hyperintense area with a corresponding increased signal on patient's DWI scan at the initial diagnostic stage and/or compatible with relevant stroke symptoms. Cortical grey matter, subcortical grey matter, white matter and cerebellum were segmented using within subject T1 intensity data and population specific probability maps, which also gives the whole brain volume.<sup>29</sup> Intracranial volume (ICV) was calculated in two stages: firstly by running FSL's Brain Extraction Tool on the GRE image from each patient; secondly, hypointense outliers (generally skull and bone in GRE) were automatically removed via Z scores. Any hypointensities within the cranial vault (e.g., microbleeds) were refilled using the MATLAB fill holes function. Finally, ICVs were checked and edited by trained image analysts (YS) and overseen by a consultant neuroradiologist (JMW).

As well as quantitative volumetrics, periventricular and deep WMH were assessed using clinical scoring with the Fazekas scale from 0-3 in deep and periventricular WMH, giving a total Fazekas score when summed out of 6.<sup>30</sup> We also rated the PVS<sup>17</sup> according to a validated semiquantitative scale from 0-4 in basal ganglia and centrum semiovale.<sup>18</sup>

#### *Flow and pulsatility measurements*

To determine flow values, we manually drew regions of interest (ROI) around ICAs, vertebral arteries, internal jugular veins, venous sinuses, aqueduct, and cervical subarachnoid spaces on images of each patient. We corrected the background phase error by carefully placing background ROIs close to but not including the studied ROIs and then subtracted the mean velocity of the background ROIs<sup>31</sup> (*Supplementary material*). The sums of the flow in ICAs and vertebral arteries on both sides gave the value of total arterial flow. The sum of the

flow in transverse sinuses and internal jugular veins on both sides represented total transverse sinus and internal jugular vein flow respectively. We calculated the CBF as mL/min and also normalised the CBF to total brain volume in order to estimate CBF per brain volume (mL/min/100 ml). For each vessel, the PI was calculated from an adapted Gosling's equation  $((\text{Flow}_{\text{maximum}} - \text{Flow}_{\text{minimum}})/\text{Flow}_{\text{mean}})$ . We also calculated a resistance index (RI) for the vessels  $((\text{Flow}_{\text{maximum}} - \text{Flow}_{\text{minimum}})/\text{Flow}_{\text{maximum}})$ .

We calculated the net CSF flow in the aqueduct and cervical subarachnoid space, by integrating positive and negative flow values in caudal and cranial directions, the stroke volume by averaging the absolute flow volume in both directions. These methods for CSF data processing were similar to those reported in a previous study.<sup>32</sup>

In order to determine the timing of pulse wave transmission through the brain, we first normalised all cardiac cycle durations to 1s (i.e. a standardised cardiac cycle), because heart rates were slightly different during the CSF and blood flow acquisitions and varied across patients. We used a similar method to that published previously.<sup>24</sup> We then measured the delay from the arterial waveform peak to the peaks in other vessels or CSF spaces in each patient. (*Figure 1*).

#### *Reproducibility analysis*

In order to test the reproducibility of the above-mentioned flow and pulsatility measures and the overall data processing methods, we also recruited 10 healthy volunteers who received two repeated phase-contrast MRI scans. Most of these measures had a good reproducibility with a within-subject coefficient of variation of less than 10% (*Details shown in Supplementary material*).

#### **Statistical analysis**

The sample size was determined to detect an effect in a similar vascular function measure called cerebrovascular reactivity (CVR), since very little data were available for PI in veins or CSF. We estimated from the literature that it would be possible to detect a relative difference in CVR of 25%, standard deviation 40%, between those with high SVD scores and low SVD scores with 80% power and alpha level 0.05. This estimated a sample size of 40 participants, however we aimed to include 60 patients to allow for technical failures or patient withdrawal from the procedure, for multivariate analysis and to increase the possibility of detecting effects on the other vascular function measures.

We performed all statistical analyses using Rstudio version 1.0.136 (RStudio Inc, Boston, MA) and SPSS version 21 (SPSS Inc, Chicago, IL). Differences in continuous variables between Fazekas groups were assessed



by analysis of variance (ANOVA), and independent sample t-tests for two-way comparisons. Differences in frequencies were compared by Chi-square tests. We used repeated measures ANOVA to compare all waveform peak delays with each other and obtained P values after Bonferroni correction for multiple comparisons.

We used linear regression models for continuous outcome variables, such as WMH as a percentage of ICV, and ordered logistic regression models for ordinal outcome variables, such as PVS score. We used CBF values that were normalised to brain volume for the following comparisons and regression models. For all regression analyses, we performed both univariate and multiple regression models with adjustment for important confounding factors or proposed predictors of SVD, including age (years) at study visit, gender and mean arterial pressure (MAP). The numbers of covariates were limited to three due to our relatively small sample size. We natural log transformed the WMH volume (%ICV) in all the linear regression models to obtain normally-distributed residuals. In all models, values of  $P < 0.05$  were considered significant.

We reported this study according to the checklist of Strengthening the Reporting of Observational Studies in Epidemiology (STROBE) statement.

## Results

### Patient characteristics (Table 1)

We recruited 60 patients, of whom 56 (40% male; mean age  $67.8 \pm 8.27$  years old, range 52 - 83) had complete MRI data. One patient did not complete the MRI scan due to claustrophobia and another due to a finding of subdural hematoma. We excluded data from another two patients because of poor peripheral pulse signal during phase-contrast MRI scans. The stroke subtype was lacunar in 36/56 and cortical in 20/56 patients. The supine blood pressure immediately after MRI scan was  $138.6 \pm 21.6 / 81.0 \pm 12.0$  mmHg. Median WMH volume was 10.7mL (range 1.4-75.0mL), representing median 0.77% (range 0.11-5.17%) of ICV. Most patients had mild to moderate SVD. In univariate comparisons, patients with higher total Fazekas score were significantly older, had more lacunes, microbleeds and higher PVS scores. There was no significant difference in gender, stroke subtype (lacunar vs cortical stroke) and other vascular risk factors between WMH severity groups.

### Summary of CBF and pulsatility measures

#### *Patients (Table 2)*

Mean total cerebral arterial flow was  $60.17 \pm 9.52$  mL/min per 100mL brain volume ( $654.32 \pm 113.00$  mL/min). Mean total transverse sinus flow was  $51.98 \pm 11.34$  per 100mL brain volume ( $562.67 \pm 117.00$  mL/min), and mean total internal jugular vein flow was  $48.12 \pm 14.82$  per 100mL brain volume ( $521.98 \pm 163.56$  mL/min). PI was highest in arteries (e.g.  $1.27 \pm 0.31$  in ICA), followed by internal jugular veins ( $0.94 \pm 0.52$ ) and lowest in venous sinuses (e.g.  $0.58 \pm 0.24$  in superior sagittal sinus). The minimum, maximum and median flow rate for each vascular waveform are provided in Supplementary Table S3. Flow waveform peak delays (with reference to arterial peak) were significantly different across veins and CSF spaces, being shortest in the cervical subarachnoid space ( $0.05 \pm 0.08$  s), followed by internal jugular veins and dural venous sinuses, and longest in the aqueduct ( $0.18 \pm 0.07$  s). There was no significant difference in any flow or pulsatility measure between patients with cortical and lacunar stroke.

#### ***Healthy volunteers (Supplementary Table S1)***

Mean total cerebral arterial flow was  $776.90 \pm 125.33$  mL/min. Mean total transverse sinus flow was  $638.62 \pm 113.78$  mL/min and mean internal jugular vein flow was  $597.47 \pm 195.05$  mL/min. PI was  $1.00 \pm 0.15$  in the ICA,  $0.57 \pm 0.30$  in the internal jugular veins, and  $0.29 \pm 0.09$  -  $0.33 \pm 0.09$  in the venous sinuses. Flow peak delays were also shortest in the cervical subarachnoid space ( $0.04 \pm 0.05$  s), followed by venous sinuses (from  $0.12 \pm 0.13$  to  $0.20 \pm 0.15$  s), and longest in the aqueduct ( $0.21 \pm 0.05$  s).

#### **Relationship between CBF, pulsatility measures and SVD features**

##### ***Univariate comparisons with WMH severity (Figure 2)***

Figure 2 shows that the PI in most vessels increased incrementally per point increase in total Fazekas score, which was statistically significant in all the venous sinuses (e.g. in superior sagittal sinus, the PI in Fazekas score groups 1-2 vs 3-4 vs 5-6 was  $0.48 \pm 0.12$  vs  $0.60 \pm 0.24$  vs  $0.73 \pm 0.32$  respectively,  $P=0.007$ ).

Internal jugular vein-to-artery and aqueduct-to-artery pulse wave peak time delays significantly decreased with increasing total Fazekas score (e.g. artery-aqueduct peak time differences by Fazekas score 1-2 vs 3-4 vs 5-6 was  $0.21 \pm 0.07$  vs  $0.17 \pm 0.06$  vs  $0.16 \pm 0.08$  s respectively,  $P=0.05$ ). Otherwise there were no significant differences in delays in other locations across Fazekas groups (*Supplementary Table S4*).

There were no significant differences of CBF across Fazekas groups. We also did not observe significant differences in CSF pulsatility measures by Fazekas group (*Supplementary Table S4*).

We also compared CBF and pulsatility measures by deep WMH (DWMH) and periventricular WMH (PVWMH) Fazekas scores separately. CBF was not associated with DWMH or PVWMH. The PI in venous sinuses increased significantly with PVWMH score (e.g. superior sagittal sinus PI  $0.48 \pm 0.14$  vs  $0.62 \pm 0.23$  vs  $0.75 \pm 0.33$  in Fazekas 1 vs 2 vs 3,  $P=0.003$ ), and increased but did not reach statistical significance with DWMH (e.g. superior sagittal sinus PI  $0.49 \pm 0.10$  vs  $0.53 \pm 0.19$  vs  $0.60 \pm 0.29$  vs  $0.71 \pm 0.27$  in Fazekas 0 vs 1 vs 2 vs 3,  $P=0.189$ ) (*Supplementary Table S5 and Table S6*).

### ***Linear regression analyses of CBF and pulsatility on WMH volume (Table 3)***

There was a weak and non-significant univariate association between lower total arterial flow and WMH volume ( $\beta=-0.024$ ,  $P=0.065$ ) (*plot A in Figure 3*), which disappeared completely when adjusted for age, gender and MAP ( $\beta=-0.018$ ,  $P=0.153$ ). There was no association between venous flow and WMH.

In univariate regression models, higher PI in the ICA ( $\beta=0.841$ ,  $P=0.038$ ) and in all venous sinuses (e.g. transverse sinus:  $\beta=1.399$ ,  $P=0.028$ ) were significantly associated with larger WMH volume (*plot B in Figure 3*). After correcting for age, gender and MAP, only higher PI in the superior sagittal and transverse sinuses remained significant (e.g. transverse sinus:  $\beta=1.364$ ,  $P=0.008$ ), but not in the ICA ( $\beta=0.435$ ,  $P=0.236$ ). There was no significant association between pulsatility in the internal jugular veins and WMH.

We did not observe any significant association between CSF pulsatility measures or waveform peak delays and WMH (*Supplementary Table S7 and Table S8*).

The associations between RI in these vessels and WMH were similar to the associations seen for PI (*Supplementary Table S9*).

In all the multiple linear regression models, older age remained a strong predictor of WMH ( $\beta \approx 0.06$ ,  $P < 0.001$ ).

### ***Ordered logistic regression analyses of CBF and pulsatility on PVS scores***

#### ***PVS in the basal ganglia (Table 4)***

In both univariate and multiple regression models, there were no associations between arterial or venous CBF and PVS in the basal ganglia, apart from a very weak association between higher internal jugular vein flow and higher PVS score (OR=1.047, 95% confidence interval (CI) [1.005, 1.09] per mL/min/100 brain volume) after adjustment for age, gender and MAP.

Higher PI in all venous sinuses, but not arteries or internal jugular veins, was significantly associated with higher PVS score in the basal ganglia, in both non-adjusted models (e.g. OR=1.532, 95%CI [1.120, 2.095] per 0.1 increase in straight sinus PI) and models adjusted for age, MAP and gender (OR=1.502, 95%CI [1.085, 2.079] per 0.1 increase in straight sinus PI). Older age was significantly associated with more PVS in all models (OR≈1.1 per year older).

There were no associations between CSF pulsatility or waveform peak delays and PVS score in the basal ganglia (*Supplementary Table S10 and S11*).

Results for RI were similar to those observed in PI (*Supplementary Table S12*).

#### *PVS in the centrum semiovale*

Apart from older age (OR≈1.1 per year older), we did not observe any associations between CBF or pulsatility in brain vessels or CSF and PVS in the centrum semiovale (*Supplementary Table S13-15*).

#### **Relationship between carotid-radial PWV, aortic AIx and SVD features (Supplementary Table S16-S18)**

Higher aortic AIx was significantly associated with higher PVS score in both the basal ganglia (OR=1.11, 95% CI [1.03, 1.22] per % increase in aortic AIx) and the centrum semiovale (OR=1.08, 95% CI [1.01, 1.16] per % increase in aortic AIx) after adjustment for age, blood pressure and gender. We did not find significant associations between aortic AIx and WMH volume, or between carotid-radial PWV and any of the SVD features after the correction for age, gender and blood pressure.

## **Discussion**

We investigated the cross-sectional relationship between CBF, intracranial pulsatility measures in cerebral arteries, veins and CSF, and SVD features, especially between these haemodynamics and PVS for the first time (summary of main results in **Figure 3**). Pulsatility in the venous sinuses increased significantly with WMH burden and basal ganglia PVS scores, independent of age, sex and MAP. Increased aortic AIx was also associated with PVS score in both basal ganglia and centrum semiovale. Shorter aqueduct- and internal jugular vein- to-artery waveform peak delays were observed in those with higher Fazekas scores, but were not associated with WMH volume or PVS scores. CSF pulsatility was not associated with WMH or PVS. Consistent with the existing literature,<sup>5</sup> we found no association between CBF and any measure of WMH. The lack of

association between CBF and PVS is a novel finding. We did not find any differences in CBF or pulsatility indices between patients with cortical and lacunar stroke, but both groups were similarly affected by SVD. These data support the concept that high cerebrovascular pulsatility is an important pathophysiological component of SVD.

The strengths of this study include recruitment of representative patients with minor stroke stratified carefully by SVD lesion burden, careful stroke classification and assessment of SVD features by specialists with standardised well-established image processing, assessment of the relationship between intracranial pulsatility and PVS for the first time, and adjustment for important confounders in the statistical analysis. Weaknesses include the sample size (n=56) that limited power for very comprehensive multivariate analysis, albeit large for a complex and the cross-sectional nature of the analysis, thus we were unable to address any causal relationship between cerebral haemodynamic and SVD. We were also not able to measure smaller vessels (e.g. penetrating arterioles) due to limited MRI resolution, or acquire independent CBF measures such as arterial spin labelling MRI. However, methods to assess PI in penetrating arterioles are currently restricted to 7T MRI and in the early stages of development and our CBF measures were consistent with known values per brain weight.

Age was prominently associated with WMH and PVS, which emphasises the importance of adjustment for age in any SVD-related analysis. The lack of association between CBF and WMH in our patients is consistent with previous evidence from large-scale cross-sectional studies and especially longitudinal studies.<sup>6, 33-35</sup> Some smaller studies did show that low CBF was associated with more WMH, but most did not account for the confounding effect of age and brain tissue loss in this relationship.<sup>5</sup> In several longitudinal studies, high baseline WMH burden predicted decreasing CBF rather than the opposite.<sup>5, 6, 35</sup> We also noticed that the blood flow in the internal jugular veins was similar to, but less than, arterial flow (ICA + vertebral arteries), which might be due to a small amount of blood draining through the extra-jugular venous systems such as vertebral, cavernous or deep neck venous plexi.<sup>36</sup>

This study is the first to observe the relationship between increased cerebrovascular (venous sinus) pulsatility and basal ganglia PVS in humans. Other indirect clinical evidence comes from a population-based study (n=1009, age 68±8 years) which showed that higher brachial pulse pressure was associated with PVS.<sup>37</sup> We also found that high PI was only associated with basal ganglia but not centrum semiovale PVS, which might reflect known differences in the arterioles in the two regions and with apparent differences in associations of PVS in the two locations, for example basal ganglia PVS may be more associated with inflammation,<sup>19</sup> hypertension<sup>38</sup> or lacunar stroke<sup>18</sup>, and centrum semiovale PVS more with cerebral amyloid angiopathy<sup>38</sup>. One mathematical

hypothetical model also suggests that in hypertension, the arteriolar pressure in the basal ganglia is higher than in cortical vessels.<sup>39</sup> However, despite the hypothetical differences in PVS in these two locations, they are strongly co-associated,<sup>40</sup> and we found PVS score in both locations to be significantly associated with aortic Aix, which is an indicator of aortic stiffness. Another explanation for the differences might be that it is more difficult to rate PVS in the centrum semiovale due to more WMH than in the basal ganglia.<sup>41</sup> Thus, before more data and more detailed studies are available, it might be too soon to conclude on the differences in the mechanisms of the two. We suggest that future studies should collect information on PVS in both sites.

The relationship between ICA pulsatility and WMH partly reflects a co-association with age and is consistent with a previous study (n=122, age 63.73±10.85 years),<sup>42</sup> but in Lothian Birth Cohort (n=694, age 72.6±0.7 years), high ICA PI remained associated with WMH after adjustment for age.<sup>13</sup> The wide age range and smaller size of our study may have made it difficult for us to untangle the confounding effect of age on ICA PI-WMH, a relationship which appears to be inherently weaker than venous PI-WMH. This may also explain the lack of association between ICA pulsatility and PVS, despite the suggestion in animal and mathematical models that arterial pulsatility is the key driver of fluid dynamics in perivascular spaces.<sup>21, 43</sup> We did not find any significant association between vertebral artery pulsatility and WMH or PVS, perhaps reflecting the low flow volume in the vertebral arteries. There were also no significant associations between carotid-radial PWV, and WMH or PVS, which might be due to different aging processes in muscular arteries compared to aorta and cerebral vessels.<sup>44</sup>

Unlike in the arteries, PI in the superior sagittal and transverse sinuses remained strongly associated with WMH independent of age and MAP. The relationship between high venous sinus pulsatility and white matter damage was also observed in patients with idiopathic dementia (n=60, age 75±8 years)<sup>32</sup> and in a healthy population (n=70, 43-82 years)<sup>12</sup>. A recent study also found that patients with Alzheimer's disease (n=26, 57-89 years) had higher venous PI compared to age-matched controls.<sup>45</sup> There is possibly a shared aetiology between WMH and PVS. PVS is associated with WMH,<sup>18</sup> and both PVS and WMH were associated with impaired blood brain barrier (BBB).<sup>46, 47</sup> High pulsatile flow along with increased sheer stress could lead to endothelial damage and deteriorate the BBB,<sup>48</sup> which might cause glial damage in the white matter. Increased pulsatility could also affect cerebral interstitial fluid drainage in perivascular spaces,<sup>21, 43</sup> thus the deposition of toxic waste product might induce brain tissue damage or blockage in the perivascular spaces, which would eventually result in WMH and increased PVS visibility. More evidence at the microscopic level is needed.

Although venous pulsatility was consistently associated with two main SVD features, its implication remains unclear. One hypothesis suggests that the systolic arterial expansion produces a pressure wave within the CSF

spaces, which is then partly transmitted into the major dural sinuses via arachnoid granulations.<sup>11</sup> Thus high venous pulsatility might indicate inefficient dampening of the arterial pulse, but how the pulse is transmitted through the older brain is largely under-researched. One study showed that the pulse transmission in the brain was from the skull base to the cortex,<sup>49</sup> similar to our findings that the waveform peak delay time from arteries was shortest in the cervical CSF, then the transverse and straight sinuses, and longest in the superior sagittal sinus. Venous pulsatility might also come partly from capillaries. Increased capillary pulsatility from less dampened arterial pulse could be transmitted to veins through blood flow or inward expansion.<sup>11</sup> However, the relationship between capillary and venous pulsatility is uncertain. As sufficient venous backpressure is important for maintaining a constant capillary flow,<sup>11</sup> venous pathologies may also result in increased capillary pulsatility, which could then cause endothelial failure and abnormalities in fluid exchange and waste product clearance via perivascular spaces.<sup>50</sup> Indeed, there are autopsy studies (n=13, age>60 years) showing collagenous thickening in periventricular venules which was associated with PVWMH severity,<sup>51</sup> but it is unknown whether the venule damage was caused by excessive pressure filtered from arteries or was an intrinsic pathology. It is likely that pathologies in arterioles and venules coexist. Future SVD studies including pathology, clinical or any models, should consider both arteries and veins.

We did not find associations between CSF stroke volume or systolic duration and SVD features. Some studies found a CSF pulsatility-WMH association<sup>52, 53</sup> but some did not<sup>12</sup>, and the indices used to represent CSF pulsatility varied. Theoretically, PVS are related to perivascular CSF dynamics driven by arterial pulsation, but the indices used here were not designed to detect this pulse at the microscopic level. There is suggestion that shorter artery-to-aqueduct peak delay might represent capillary dysfunction in patients with late-life depression and high WMH burden,<sup>22</sup> but we did not find associations between any peak delays and WMH volume. 2D phase-contrast MRI has limited temporal resolution and the reliability of the pulse wave peak delays still requires more research. Further research would benefit from improved imaging techniques with high temporal and spatial resolution to detect small vessels in more detail, and intracranial pulsation with higher sensitivity.

## Conclusions

We did not find significant association between CBF and SVD features in this cross-sectional study. However, WMH and basal ganglia PVS are closely associated with increased cerebrovascular pulsatility, especially in the venous sinuses, which suggests alternative mechanisms rather than just low CBF in SVD. Although the

implication of venous sinus pulsatility requires further research, this study has measured the pulse wave from the main arteries to the veins and CSF spaces in the brain, as well as confirming that increased intracranial (particularly venous) pulsatility is important in the pathogenesis of SVD, thus identifying potential targets for future mechanistic studies, treatment and prevention of SVD.

## Acknowledgements

This work was funded by the Chief Scientist Office of Scotland (grant ETM/326), the Wellcome Trust-University of Edinburgh Institutional Strategic Support Fund, the Scottish Imaging Network: A Platform for Scientific Excellence (“SINAPSE”, funded by the Scottish Funding Council and the Chief Scientist Office of Scotland), the China Scholarship Council (Y.S.), National Health Service (NHS) Lothian Research and Development Office (M.J.T), the Alzheimer’s Society (grant ref AS-PG-14-033; G.B.), Edinburgh and Lothian Trust Fund (G.B.), Stroke Association/Garfield Weston Foundation Senior Clinical Fellowship (F.D.), NHS Research Scotland Fellow (F.D.), Innovate UK (D.A.D.), the Medical Research Council through the Centre for Cognitive Ageing and Cognitive Epidemiology (CCACE), the Fondation Leducq Network for the Study of Perivascular Spaces in Small Vessel Disease (ref no. 16 CVD 05), and European Union Horizon 2020, PHC-03-15, project No 666881, ‘SVDs@Target’. Once the primary papers are published, data will be available via the Cerebrovascular Diseases Databank at the University of Edinburgh and can be accessed by approaching the authors.

## Author Contributions

J.W., I.M., M.T., F.D., F.C., and G.B. were responsible for study concept and design. All authors were responsible for data acquisition and analysis. Y.S., M.T., G.B., D.A.D., I.M., and J.W. were responsible for drafting the manuscript and figures.

## Conflicts of Interest

No.



1

2   Supplementary material for this paper is available at: <http://jcbfm.sagepub.com/content/by/supplementary-data>.

3

## References

1. DeBette S and Markus HS. The clinical importance of white matter hyperintensities on brain magnetic resonance imaging: systematic review and meta-analysis. *BMJ*. 2010; 341: c3666.
2. Vermeer SE, Longstreth WT, Jr. and Koudstaal PJ. Silent brain infarcts: a systematic review. *Lancet Neurol*. 2007; 6: 611-9.
3. Wen W and Sachdev PS. Extent and distribution of white matter hyperintensities in stroke patients: the Sydney Stroke Study. *Stroke*. 2004; 35: 2813-9.
4. Gorelick PB, Scuteri A, Black SE, et al. Vascular contributions to cognitive impairment and dementia: a statement for healthcare professionals from the american heart association/american stroke association. *Stroke*. 2011; 42: 2672-713.
5. Shi Y, Thrippleton MJ, Makin SD, et al. Cerebral blood flow in small vessel disease: A systematic review and meta-analysis. *J Cereb Blood Flow Metab*. 2016; 36: 1653-67.
6. van der Veen PH, Muller M, Vincken KL, et al. Longitudinal relationship between cerebral small-vessel disease and cerebral blood flow: the second manifestations of arterial disease-magnetic resonance study. *Stroke*. 2015; 46: 1233-8.
7. de Roos A, van der Grond J, Mitchell G and Westenberg J. Magnetic Resonance Imaging of Cardiovascular Function and the Brain: Is Dementia a Cardiovascular-Driven Disease? *Circulation*. 2017; 135: 2178-95.
8. O'Rourke MF and Hashimoto J. Mechanical factors in arterial aging: a clinical perspective. *J Am Coll Cardiol*. 2007; 50: 1-13.
9. Benetos A, Waeber B, Izzo J, et al. Influence of age, risk factors, and cardiovascular and renal disease on arterial stiffness: clinical applications. *Am J Hypertens*. 2002; 15: 1101-8.
10. Mitchell GF. Cerebral small vessel disease: role of aortic stiffness and pulsatile hemodynamics. *J Hypertens*. 2015; 33: 2025-8.
11. Stivaros SM and Jackson A. Changing concepts of cerebrospinal fluid hydrodynamics: role of phase-contrast magnetic resonance imaging and implications for cerebral microvascular disease. *Neurotherapeutics*. 2007; 4: 511-22.
12. Jolly TA, Bateman GA, Levi CR, Parsons MW, Michie PT and Karayanidis F. Early detection of microstructural white matter changes associated with arterial pulsatility. *Front Hum Neurosci*. 2013; 7: 782.
13. Aribisala BS, Morris Z, Eadie E, et al. Blood pressure, internal carotid artery flow parameters, and age-related white matter hyperintensities. *Hypertension*. 2014; 63: 1011-8.
14. Webb AJ, Simoni M, Mazzucco S, Kuker W, Schulz U and Rothwell PM. Increased cerebral arterial pulsatility in patients with leukoaraiosis: arterial stiffness enhances transmission of aortic pulsatility. *Stroke*. 2012; 43: 2631-6.
15. Shi Y, Thrippleton MJ, Marshall I and Wardlaw JM. Intracranial pulsatility in patients with cerebral small vessel disease: a systematic review. *Clin Sci (Lond)*. 2017.
16. Bateman GA, Levi CR, Schofield P, Wang Y and Lovett EC. The venous manifestations of pulse wave encephalopathy: windkessel dysfunction in normal aging and senile dementia. *Neuroradiology*. 2008; 50: 491-7.
17. Wardlaw JM, Smith EE, Biessels GJ, et al. Neuroimaging standards for research into small vessel disease and its contribution to ageing and neurodegeneration. *Lancet Neurol*. 2013; 12: 822-38.
18. Doubal FN, MacLulich AM, Ferguson KJ, Dennis MS and Wardlaw JM. Enlarged perivascular spaces on MRI are a feature of cerebral small vessel disease. *Stroke*. 2010; 41: 450-4.
19. Aribisala BS, Wiseman S, Morris Z, et al. Circulating inflammatory markers are associated with magnetic resonance imaging-visible perivascular spaces but not directly with white matter hyperintensities. *Stroke*. 2014; 45: 605-7.
20. Shi Y and Wardlaw J. Update on cerebral small vessel disease: a dynamic whole-brain disease. *Stroke and Vascular Neurology*. 2016; 2: 83-92.
21. Iliff JJ, Wang M, Zeppenfeld DM, et al. Cerebral arterial pulsation drives paravascular CSF-interstitial fluid exchange in the murine brain. *J Neurosci*. 2013; 33: 18190-9.
22. Naish JH, Baldwin RC, Patankar T, et al. Abnormalities of CSF flow patterns in the cerebral aqueduct in treatment-resistant late-life depression: a potential biomarker of microvascular angiopathy. *Magn Reson Med*. 2006; 56: 509-16.
23. Stoquart-Elsankari S, Lehmann P, Villette A, et al. A phase-contrast MRI study of physiologic cerebral venous flow. *J Cereb Blood Flow Metab*. 2009; 29: 1208-15.
24. Stoquart-Elsankari S, Baledent O, Gondry-Jouet C, Makki M, Godefroy O and Meyer ME. Aging effects on cerebral blood and cerebrospinal fluid flows. *J Cereb Blood Flow Metab*. 2007; 27: 1563-72.

25. Thrippleton MJ, Shi Y, Blair G, et al. Cerebrovascular reactivity measurement in cerebral small vessel disease: rationale and reproducibility of a protocol for MRI acquisition and image processing. *International Journal of Stroke*. In Press.
26. Jenkinson M and Smith S. A global optimisation method for robust affine registration of brain images. *Med Image Anal*. 2001; 5: 143-56.
27. Avants BB, Epstein CL, Grossman M and Gee JC. Symmetric diffeomorphic image registration with cross-correlation: evaluating automated labeling of elderly and neurodegenerative brain. *Med Image Anal*. 2008; 12: 26-41.
28. Freedman D, Pisani R and Purves R. *Statistics*. New York: W. W. Norton, 2007.
29. Avants BB, Tustison NJ, Wu J, Cook PA and Gee JC. An open source multivariate framework for n-tissue segmentation with evaluation on public data. *Neuroinformatics*. 2011; 9: 381-400.
30. Fazekas F, Chawluk JB, Alavi A, Hurtig HI and Zimmerman RA. MR signal abnormalities at 1.5 T in Alzheimer's dementia and normal aging. *AJR Am J Roentgenol*. 1987; 149: 351-6.
31. Walker PG, Cranney GB, Scheidegger MB, Waseleski G, Pohost GM and Yoganathan AP. Semiautomated method for noise reduction and background phase error correction in MR phase velocity data. *J Magn Reson Imaging*. 1993; 3: 521-30.
32. Bateman GA. Pulse-wave encephalopathy: A comparative study of the hydrodynamics of leukoaraiosis and normal-pressure hydrocephalus. *Neuroradiology*. 2002; 44: 740-8.
33. Vernooij MW, van der Lugt A, Ikram MA, et al. Total cerebral blood flow and total brain perfusion in the general population: the Rotterdam Scan Study. *J Cereb Blood Flow Metab*. 2008; 28: 412-9.
34. van Es AC, van der Grond J, ten Dam VH, et al. Associations between total cerebral blood flow and age related changes of the brain. *PLoS One*. 2010; 5: e9825.
35. Nylander R, Fahlstrom M, Rostrup E, et al. Quantitative and qualitative MRI evaluation of cerebral small vessel disease in an elderly population: a longitudinal study. *Acta Radiol*. 2017; 284185117727567.
36. Doepp F, Schreiber SJ, von Munster T, Rademacher J, Klingebiel R and Valdueza JM. How does the blood leave the brain? A systematic ultrasound analysis of cerebral venous drainage patterns. *Neuroradiology*. 2004; 46: 565-70.
37. Gutierrez J, Elkind MS, Cheung K, Rundek T, Sacco RL and Wright CB. Pulsatile and steady components of blood pressure and subclinical cerebrovascular disease: the Northern Manhattan Study. *J Hypertens*. 2015; 33: 2115-22.
38. Yakushiji Y, Charidimou A, Hara M, et al. Topography and associations of perivascular spaces in healthy adults: the Kashima scan study. *Neurology*. 2014; 83: 2116-23.
39. Blanco PJ, Müller LO and Spence JD. Blood pressure gradients in cerebral arteries: a clue to pathogenesis of cerebral small vessel disease. *stroke and Vascular Neurology*. 2017; 2: e000087.
40. Potter GM, Doubal FN, Jackson CA, et al. Enlarged perivascular spaces and cerebral small vessel disease. *Int J Stroke*. 2015; 10: 376-81.
41. Potter GM, Chappell FM, Morris Z and Wardlaw JM. Cerebral perivascular spaces visible on magnetic resonance imaging: development of a qualitative rating scale and its observer reliability. *Cerebrovasc Dis*. 2015; 39: 224-31.
42. Tanaka T, Shimizu T and Fukuhara T. The relationship between leukoaraiosis volume and parameters of carotid artery duplex ultrasonographic scanning in asymptomatic diabetic patients. *Computerized Medical Imaging and Graphics*. 2009; 33: 489-93.
43. Bilston LE, Fletcher DF, Brodbelt AR and Stoodley MA. Arterial pulsation-driven cerebrospinal fluid flow in the perivascular space: a computational model. *Comput Methods Biomech Biomed Engin*. 2003; 6: 235-41.
44. Mitchell GF. Effects of central arterial aging on the structure and function of the peripheral vasculature: implications for end-organ damage. *J Appl Physiol (1985)*. 2008; 105: 1652-60.
45. Rivera-Rivera LA, Schubert T, Turski P, et al. Changes in intracranial venous blood flow and pulsatility in Alzheimer's disease: A 4D flow MRI study. *J Cereb Blood Flow Metab*. 2017; 37: 2149-58.
46. Wardlaw JM, Doubal F, Armitage P, et al. Lacunar stroke is associated with diffuse blood-brain barrier dysfunction. *Ann Neurol*. 2009; 65: 194-202.
47. Starr JM, Wardlaw J, Ferguson K, MacLulich A, Deary IJ and Marshall I. Increased blood-brain barrier permeability in type II diabetes demonstrated by gadolinium magnetic resonance imaging. *J Neurol Neurosurg Psychiatry*. 2003; 74: 70-6.
48. Garcia-Polite F, Martorell J, Del Rey-Puech P, et al. Pulsatility and high shear stress deteriorate barrier phenotype in brain microvascular endothelium. *J Cereb Blood Flow Metab*. 2017; 37: 2614-25.
49. Kiviniemi V, Wang X, Korhonen V, et al. Ultra-fast magnetic resonance encephalography of physiological brain activity - Glymphatic pulsation mechanisms? *J Cereb Blood Flow Metab*. 2016; 36: 1033-45.

- 1 50. Mestre H, Kostrikov S, Mehta RI and Nedergaard M. Perivascular spaces, glymphatic dysfunction, and  
2 small vessel disease. *Clin Sci (Lond)*. 2017; 131: 2257-74.
- 3 51. Moody DM, Brown WR, Challa VR and Anderson RL. Periventricular venous collagenosis:  
4 association with leukoaraiosis. *Radiology*. 1995; 194: 469-76.
- 5 52. Beggs CB, Magnano C, Shepherd SJ, et al. Dirty-Appearing White Matter in the Brain is Associated  
6 with Altered Cerebrospinal Fluid Pulsatility and Hypertension in Individuals without Neurologic Disease.  
7 *Journal of Neuroimaging*. 2016; 26: 136-43.
- 8 53. Henry-Feugeas MC, Roy C, Baron G and Schouman-Claeys E. Leukoaraiosis and pulse-wave  
9 encephalopathy: Observations with phase-contrast MRI in mild cognitive impairment. *Journal of*  
10 *Neuroradiology*. 2009; 36: 212-8.

11

12

## Figure legends

**Figure 1** Sagittal cross section of the head showing the locations sampled with phase-contrast MRI, and example flow waveforms of selected vessels and cerebrospinal fluid (CSF) spaces (yellow) in one standardised cardiac cycle. Thick color lines on the sagittal image indicate the locations of slices for phase-contrast MRI scans. Arrows indicate the directions of flow. In each waveform, dashed lines in the same colour as the flow curve point to the time of peak flow, while red dashed lines in all waveforms show the time of arterial peak flow. For the arterial flow waveform, we combined the flow from both internal carotid arteries (ICA) and both vertebral arteries in this example, but we calculated pulsatility index (PI) for the ICAs and vertebral arteries separately in the analyses. A: arteries including both ICA and vertebral arteries; B: superior sagittal sinus; C: straight sinus; D: transverse sinus; E: internal jugular vein; F: cerebral aqueduct; G: cervical subarachnoid space.

**Figure 2** Boxplot showing the univariate comparisons of pulsatility index in the arteries to veins according to total Fazekas score. P values were from ANOVA and were marked bold when less than 0.05. Sample sizes in each group: Fazekas 1-2 (n=24); 3-4 (n=19); 5-6 (n=13). ICA: internal carotid artery.

**Figure 3** Schematic summary of main results with representative plots. Since it is difficult to plot multivariable models, we used univariate plots instead, but the trends of the results were consistent with those from multivariable models. The four plots in the right panel include scatterplots for associations of WMH volume/ICV ratio with total arterial flow (A) and with PI in superior sagittal sinus (B), and boxplots for associations of basal ganglia PVS score with total arterial flow (C) and with superior sagittal sinus PI (D).  $\beta$  coefficients and p values in scatterplots were from univariate regression models, in which WMH volume/ICV was natural logged due to non-normally distributed residuals in the models. P values in boxplots were from univariate comparisons of the above-mentioned haemodynamics between PVS score groups. We also summarised the main results from multivariable models in the bottom left panel of this figure. SVD: small vessel disease; WMH: white matter hyperintensities; ICV: intracranial volume; PI: pulsatility index; BG: basal ganglia; PVS: perivascular spaces; CBF: cerebral blood flow; ICA: internal carotid artery.

Table 1 Summary of patient characteristics and univariate comparisons between Fazekas score groups

	Total Fazekas score			P value	Overall (n=56)
	1-2 (n=24)	3-4 (n=19)	5-6 (n=13)		
Mean age (s.d.), yr	<b>64.25 (7.76)</b>	<b>69.11 (7.11)</b>	<b>72.46 (8.39)</b>	<b>&lt;0.01</b>	67.80 (8.27)
Male, n (%)	17 (70.80)	14 (73.70)	9 (69.20)	0.96	40 (71.40)
Lacunar stroke*, n (%)	13 (54.20)	13 (68.40)	10 (76.90)	0.35	36 (64.30)
History of stroke, n (%)	3 (12.50)	1 (5.30)	2 (15.40)	0.62	6 (10.70)
Diabetes, n (%)	3 (12.50)	2 (10.50)	2 (15.40)	0.92	7 (12.50)
AF, n (%)	0	3 (15.80)	2 (15.40)	0.13	5 (8.90)
Hyperlipidaemia, n (%)	14 (58.30)	12 (63.20)	11 (84.60)	0.26	37 (66.10)
Hypertension, n (%)	18 (75.00)	15 (78.90)	9 (69.20)	0.82	42 (75.00)
Mean systolic BP (s.d.), mmHg	135.91 (20.64)	137.95 (22.75)	144.38 (22.17)	0.53	138.62 (21.60)
Mean diastolic BP (s.d.), mmHg	80.91 (12.60)	78.00 (11.84)	85.62 (10.66)	0.22	81.02 (12.04)
Use anti-hypertensive drugs (%)	11 (45.80)	12 (63.20)	8 (61.50)	0.46	31 (55.40)
Use statins (%)	24 (100.0)	16 (84.20)	11 (84.60)	0.13	51 (91.10)
Use anti-platelets (%)	23 (95.80)	17 (89.50)	11 (84.60)	0.50	51 (91.10)
Presence of lacune, n (%)	<b>10 (41.70)</b>	<b>12 (63.20)</b>	<b>13 (100.00)</b>	<b>&lt;0.01</b>	35 (62.50)
Presence of CMB, n (%)	<b>0</b>	<b>3 (15.80)</b>	<b>5 (38.50)</b>	<b>&lt;0.01</b>	8 (14.30)
Mean intracranial volume (s.d.), mL	1479.07 (123.78)	1490.42 (147.60)	1461.18 (142.46)	0.84	1478.77 (134.48)
Median WMH volume [range], mL	<b>5.25 [4.05, 7.54]</b>	<b>12.84 [10.32, 0.61]</b>	<b>44.29 [24.60, 3.10]</b>	<b>&lt;0.01</b>	10.74 [1.40, 74.97]
Median WMH/ICV [range], %	<b>0.37 [0.27, 0.49]</b>	<b>0.99 [0.69, 1.27]</b>	<b>2.96 [1.63, 3.90]</b>	<b>&lt;0.01</b>	0.77 [0.11, 5.17]
Median PVWMH Fazekas [range]	1 [1, 1]	2 [1, 2]	3 [2, 3]	<b>&lt;0.01</b>	2 [1, 3]
Median DWMH Fazekas [range]	1 [0, 1]	2 [1, 2]	3 [2, 3]	<b>&lt;0.01</b>	1 [0, 3]
Median basal ganglia PVS score [range]	1 [1, 3]	2 [1, 3]	3 [1, 4]	<b>0.01</b>	2 [1, 4]
Median centrum semiovale PVS score [range]	2 [1, 3]	3 [1, 4]	3 [1, 4]	0.05	2.5 [1, 4]

s.d.: standard deviation; AF: Atrial fibrillation; BP: blood pressure; CMB: cerebral microbleeds; PVWMH: periventricular white matter hyperintensities; DWMH: deep white matter hyperintensities; PVS: perivascular spaces; WMH: white matter hyperintensities; ICV: intracranial volume. P values were from ANOVA for continuous variable and from Chi-square test for proportions. Bold text indicates results with p <0.05. \*Lacunar stroke (vs cortical stroke).

Table 2 Summary of flow and pulsatility indices and univariate comparisons between stroke subtypes

	Overall (n=56) Mean (s.d.)	Cortical Stroke (n=20) Mean (s.d.)	Lacunar stroke (n=36) Mean (s.d.)	P value
Total arterial flow (mL/min)	654.32 (113.00)	625.67 (119.14)	670.23 (107.84)	0.16
Total arterial flow (mL/min/100mL brain volume)	60.17 (9.52)	58.59 (10.86)	61.05 (8.72)	0.36
Total transverse sinus flow (mL/min)	562.67 (117.00)	577.41 (132.64)	554.48 (108.47)	0.49
Total transverse sinus flow (mL/min/100mL brain volume)	51.98 (11.34)	54.42 (13.59)	50.62 (9.82)	0.23
Total internal jugular flow (mL/min)	521.98 (163.56)	514.67 (107.70)	526.04 (188.94)	0.81
Total internal jugular flow (mL/min/100mL brain volume)	48.12 (14.82)	48.15 (10.01)	48.11 (17.05)	0.99
ICA PI	1.27 (0.31)	1.27 (0.34)	1.27 (0.29)	0.98
Vertebral artery PI	1.48 (0.38)	1.51 (0.49)	1.46 (0.31)	0.62
Superior sagittal sinus PI	0.58 (0.24)	0.57 (0.28)	0.59 (0.22)	0.77
Straight sinus PI	0.52 (0.19)	0.48 (0.21)	0.54 (0.18)	0.28
Transverse sinus PI	0.53 (0.21)	0.50 (0.22)	0.55 (0.21)	0.42
Internal jugular vein PI	0.94 (0.52)	0.85 (0.38)	0.99 (0.59)	0.35
Net aqueduct CSF flow (mL/min)*	0.20 (0.78)	0.20 (0.68)	0.24 (0.76)	0.84
Aqueduct stroke volume (mL)	0.06 (0.04)	0.06 (0.05)	0.05 (0.03)	0.29
Duration of systolic phase in aqueduct (s)	0.46 (0.07)	0.47 (0.06)	0.45 (0.08)	0.45
Net cervical CSF flow (mL/min)*	-1.68 (4.25)	-2.72 (3.65)	-1.10 (4.50)	0.17
Cervical CSF stroke volume (mL)	0.48 (0.21)	0.49 (0.22)	0.47 (0.21)	0.78
Duration of systolic phase in cervical CSF (s)	0.36 (0.07)	0.36 (0.05)	0.36 (0.08)	0.96
Waveform peak delays with reference to arterial waveform peak (s) in				
Superior sagittal sinus	0.16 (0.10)	0.17 (0.12)	0.16 (0.09)	0.82
Straight sinus	0.13 (0.11)	0.10 (0.09)	0.14 (0.11)	0.14
Transverse sinus	0.12 (0.09)	0.10 (0.10)	0.13 (0.09)	0.33
Internal jugular veins	0.11 (0.10)	0.11 (0.09)	0.11 (0.11)	0.84
Aqueduct CSF	0.18 (0.07)	0.19 (0.07)	0.18 (0.07)	0.58
Cervical CSF	0.04 (0.08)	0.04 (0.08)	0.05 (0.08)	0.74
Peripheral arterial measurements				
Carotid-radial PWV (m/s)	8.16 (1.92)	7.87 (1.86)	8.11 (1.76)	0.63

	Aortic augmentation index (%)	24.81 (9.61)	26.90 (11.96)	23.65 (8.13)	0.23
1	CBF: cerebral blood flow; s.d.: standard deviation; ICA: internal carotid arteries; PWV: pulse wave velocity; PI: pulsatility index; CSF: cerebrospinal fluid. P				
2	values were from independent-sample t-test. *for the net CSF flow in the aqueduct and the cervical subarachnoid spaces, positive value indicates flow at the				
3	caudal direction, whereas negative value indicates flow at the cranial direction.				



1  
2

Table 3 Association of CBF, cerebrovascular pulsatility with WMH

ln WMH volume/ICV ratio as outcome (linear regression)							
Univariate linear regression models				Multiple linear regression models			
Predictors	$\beta$	95% CI	P value	Predictors	$\beta$	95% CI	P value
Total arterial flow*	-0.02	[-0.05, 0]	0.07	Total arterial flow*	-0.02	[-0.04, 0.01]	0.15
				<b>Age</b>	<b>0.06</b>	<b>[0.03, 0.08]</b>	<b>&lt;0.01</b>
				MAP	0.01	[-0.01, 0.03]	0.16
				Gender	0.03	[-0.46, 0.52]	0.15
Total transverse sinus flow*	-0.01	[-0.03, 0.01]	0.40	Total transverse sinus flow*	-0.01	[-0.03, 0.01]	0.34
				<b>Age</b>	<b>0.06</b>	[0.03, 0.09]	<b>&lt;0.01</b>
				MAP	0.01	[-0.01, 0.02]	0.28
				Gender	-0.06	[-0.64, 0.52]	0.83
Total internal jugular vein flow*	-0.01	[-0.03, 0.01]	0.17	Total internal jugular vein flow*	<0.01	[-0.02, 0.01]	0.57
				<b>Age</b>	<b>0.06</b>	<b>[0.03, 0.09]</b>	<b>&lt;0.01</b>
				MAP	0.01	[-0.01, 0.02]	0.29
				Gender	0.06	[-0.45, 0.57]	0.82
<b>ICA PI</b>	<b>0.84</b>	<b>[0.05, 1.63]</b>	<b>0.04</b>	ICA PI	0.44	[-0.29, 1.16]	0.24
				<b>Age</b>	<b>0.06</b>	<b>[0.03, 0.09]</b>	<b>&lt;0.01</b>
				MAP	0.01	[-0.01, 0.02]	0.37
				Gender	0.06	[-0.43, 0.55]	0.80
Vertebral artery PI	0.33	[-0.32, 0.99]	0.31	Vertebral artery PI	0.10	[-0.49, 0.67]	0.76
				<b>Age</b>	<b>0.06</b>	<b>[0.03, 0.09]</b>	<b>&lt;0.01</b>
				MAP	0.29	[-0.01, 0.02]	0.29
				Gender	0.08	[-0.42, 0.58]	0.74
<b>Superior sagittal sinus PI</b>	<b>1.59</b>	<b>[0.64, 2.55]</b>	<b>&lt;0.01</b>	<b>Superior sagittal sinus PI</b>	<b>1.29</b>	<b>[0.40, 2.17]</b>	<b>&lt;0.01</b>
				<b>Age</b>	<b>0.06</b>	<b>[0.03, 0.08]</b>	<b>&lt;0.01</b>
				MAP	0.01	[-0.01, 0.02]	0.21

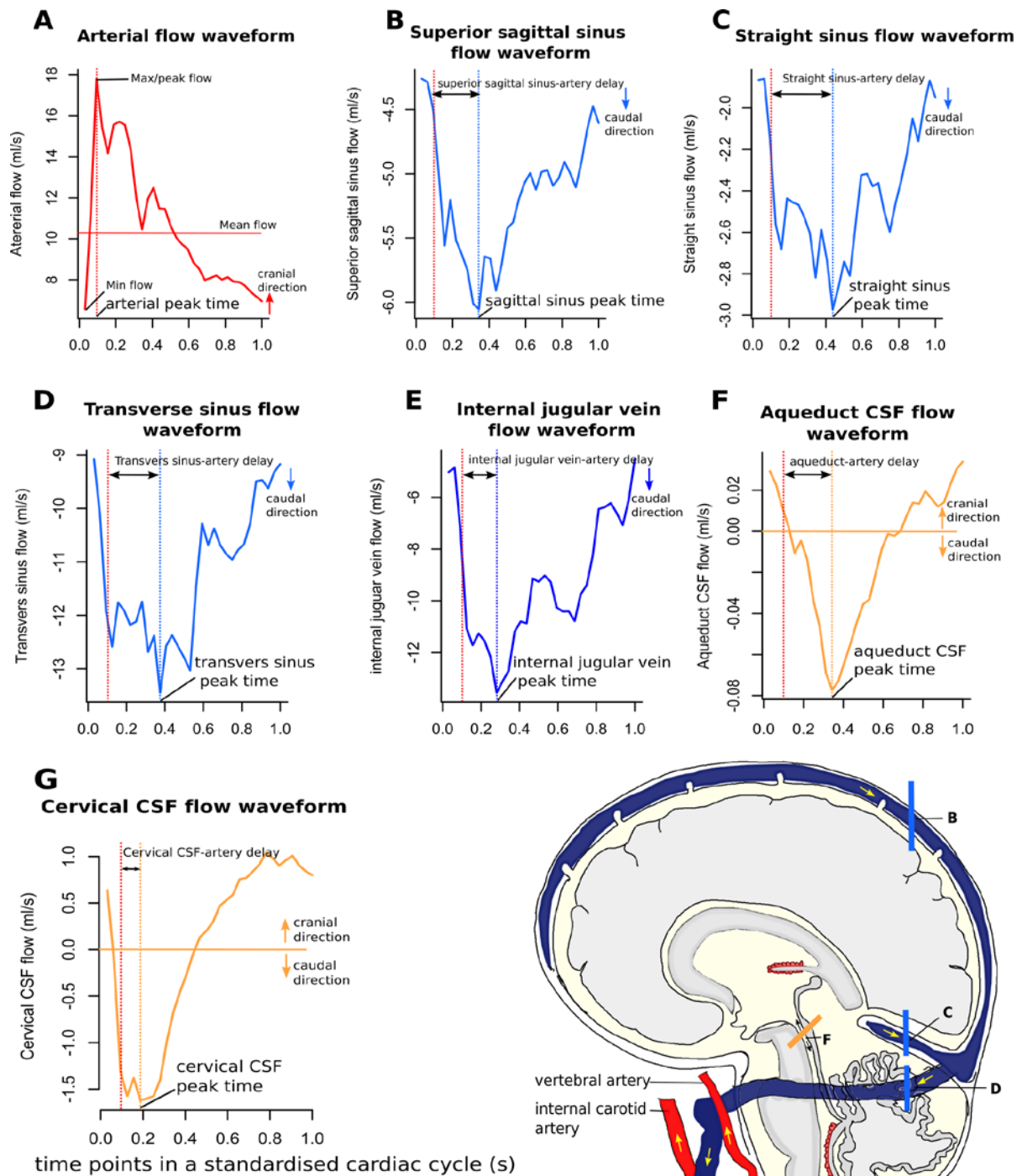
				Gender	0.24	[-0.23, 0.72]	0.30
<b>Straight sinus PI</b>	<b>1.40</b>	<b>[0.16, 2.64]</b>	<b>0.03</b>	Straight sinus PI	0.90	[-0.31, 2.11]	0.14
				<b>Age</b>	<b>0.06</b>	<b>[0.03, 0.08]</b>	<b>&lt;0.01</b>
				MAP	0.01	[-0.01, 0.03]	0.16
				Gender	0.15	[-0.34, 0.64]	0.54
<b>Transverse sinus PI</b>	<b>1.65</b>	<b>[0.55, 2.76]</b>	<b>&lt;0.01</b>	<b>Transverse sinus PI</b>	<b>1.36</b>	<b>[0.37, 2.36]</b>	<b>&lt;0.01</b>
				<b>Age</b>	<b>0.06</b>	<b>[0.03, 0.08]</b>	<b>&lt;0.01</b>
				MAP	0.01	[-0.01, 0.03]	0.17
				Gender	0.20	[-0.27, 0.67]	0.40
Internal jugular vein PI	0.10	[-0.38, 0.58]	0.67	Internal jugular vein PI	0.204	[-0.23, 0.64]	0.35
				<b>Age</b>	<b>0.062</b>	<b>[0.04, 0.09]</b>	<b>&lt;0.01</b>
				MAP	0.011	[-0.01, 0.03]	0.20
				Gender	0.106	[-0.39, 0.60]	0.67

- 1 WMH: white matter hyperintensities; ICV: intracranial volume; MAP: mean arterial pressure; ICA: internal carotid artery; PI: pulsatility index. Bold text indicates results with p < 0.05. WMH/ICV ratio was natural log transformed in all models due to non-normal distribution. \*Unit of cerebral blood flow: mL/min/(100mL brain volume)
- 2

Table 4 Association of CBF and cerebrovascular pulsatility with basal ganglia PVS

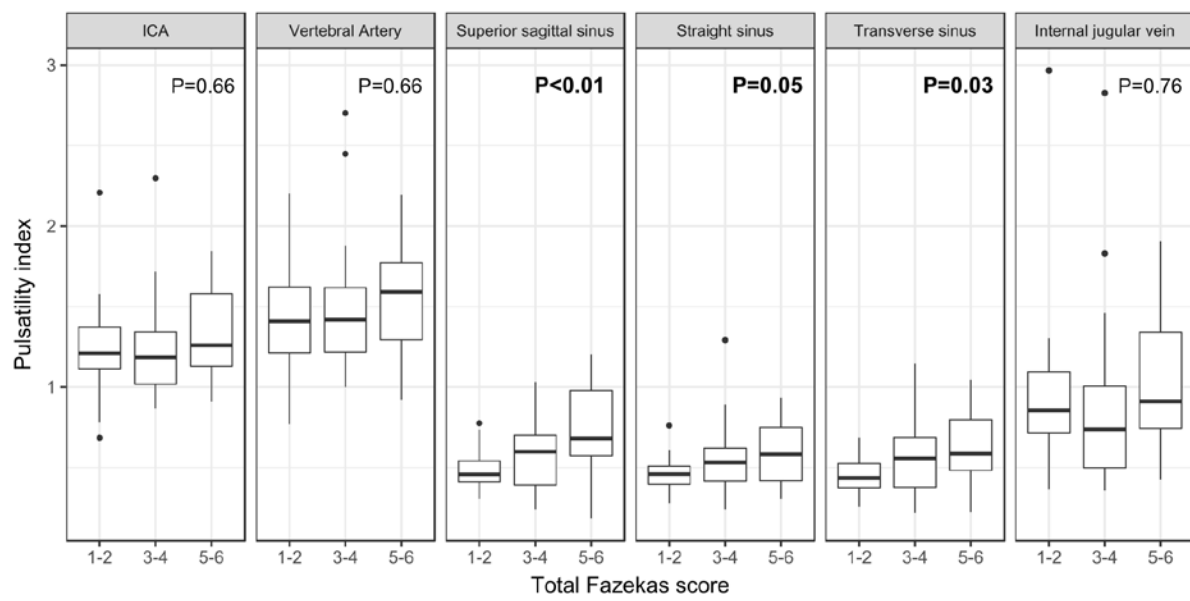
<b>PVS score in basal ganglia as outcome (ordered logistic regression)</b>					
Univariate regression models			Multiple regression models		
Predictors	OR	95% CI	Predictors	OR	95% CI
Total arterial flow (per mL/min/100mL brain volume)	1.03	[0.97, 1.08]	Total arterial flow	1.07	[1.00, 1.14]
			<b>Age (per year)</b>	<b>1.14</b>	<b>[1.06, 1.23]</b>
			MAP (per mmHg)	1.02	[0.98, 1.05]
			Gender (male)	1.17	[0.36, 3.84]
Total Transverse sinus flow (per mL/min/100mL brain volume)	1.01	[0.97, 1.06]	Total Transverse sinus flow	1.03	[0.98, 1.09]
			<b>Age</b>	<b>1.12</b>	<b>[1.04, 1.20]</b>
			MAP	1.03	[0.99, 1.06]
			Gender (male)	1.46	[0.38, 5.65]
Total Internal jugular vein flow (per mL/min/100mL brain volume)	1.02	[0.99, 1.05]	<b>Total Internal jugular vein flow</b>	<b>1.05</b>	<b>[1.01, 1.09]</b>
			<b>Age</b>	<b>1.14</b>	<b>[1.06, 1.23]</b>
			MAP	1.02	[0.99, 1.06]
			Gender	1.44	[0.43, 4.83]
ICA PI (per 0.1)	1.08	[0.93, 1.26]	ICA PI	1.00	[0.85, 1.18]
			<b>Age (per year)</b>	<b>1.11</b>	<b>[1.03, 1.19]</b>
			MAP (per mmHg)	1.02	[0.98, 1.06]
			Gender (male)	0.99	[0.32, 3.11]
Vertebral artery PI (per 0.1)	1.01	[0.89, 1.15]	Vertebral artery PI	0.96	[0.83, 1.10]
			<b>Age</b>	<b>1.11</b>	<b>[1.04, 1.19]</b>
			MAP	1.02	[0.99, 1.06]
			Gender	1.03	[0.32, 3.26]
<b>Superior sagittal sinus PI (per 0.1)</b>	<b>1.42</b>	<b>[1.11, 1.81]</b>	<b>Superior sagittal sinus PI</b>	<b>1.38</b>	<b>[1.06, 1.80]</b>
			<b>Age</b>	<b>1.09</b>	<b>[1.02, 1.17]</b>
			MAP	1.03	[0.99, 1.07]
			Gender	1.56	[0.46, 5.30]
<b>Straight sinus PI (per 0.1)</b>	<b>1.53</b>	<b>[1.12, 2.10]</b>	<b>Straight sinus PI</b>	<b>1.50</b>	<b>[1.09, 2.08]</b>
			<b>Age</b>	<b>1.08</b>	<b>[1.01, 1.16]</b>
			MAP	1.04	[1.00, 1.08]
			Gender	1.48	[0.44, 4.97]
<b>Transverse sinus PI (per 0.1)</b>	<b>1.44</b>	<b>[1.11, 1.88]</b>	<b>Transverse sinus PI</b>	<b>1.43</b>	<b>[1.09, 1.87]</b>
			<b>Age</b>	<b>1.10</b>	<b>[1.03, 1.18]</b>
			MAP	1.03	[0.99, 1.07]
			Gender	1.39	[0.42, 4.62]
Internal jugular vein PI (per 0.1)	1.01	[0.91, 1.11]	Internal jugular vein PI	1.03	[0.92, 1.16]
			<b>Age</b>	<b>1.11</b>	<b>[1.04, 1.19]</b>
			MAP	1.03	[0.99, 1.06]
			Gender	1.04	[0.33, 3.30]

1 CBF: cerebral blood flow; PVS: perivascular spaces; OR: odds ratio; CI: confidence interval; PI: pulsatility  
2 index; MAP: mean arterial pressure. Bold text indicates results that do not overlap with the null value (OR=1).  
3



1  
2

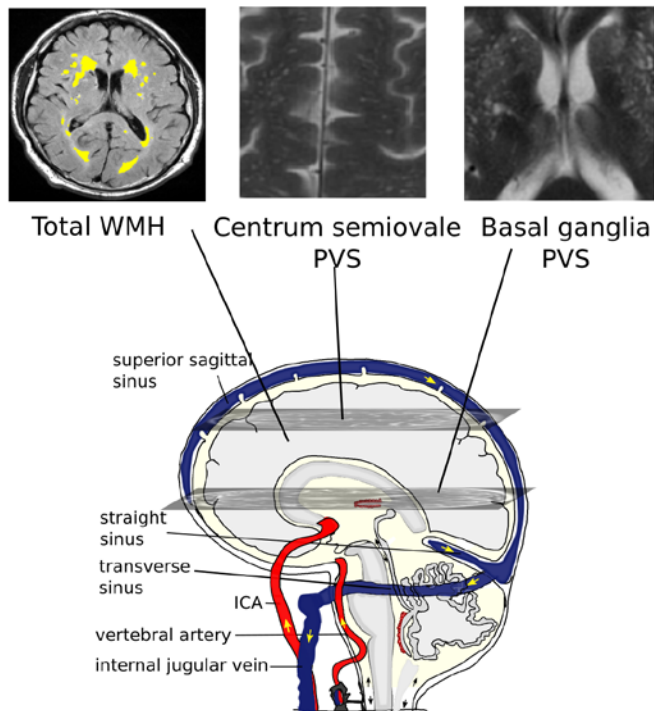
1



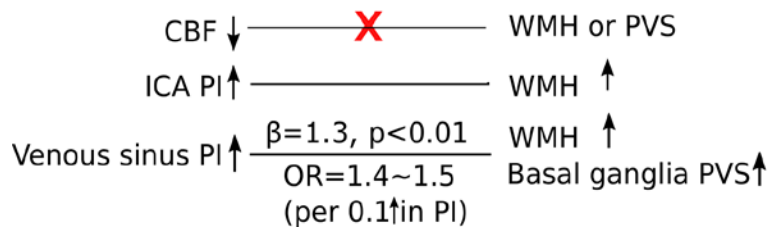
2

3

1



### Summary of results from multivariable models



2

### Representative univariate plots

